C. R. Chimie 19 (2016) 496–504

Contents lists available at ScienceDirect

Comptes Rendus Chimie

www.sciencedirect.com

Full paper/Mémoire

# Design and characterization of flat membrane supports elaborated from kaolin and aluminum powders

## *Élaboration et caractérisation de supports membranaires plans à base de kaolin et d'aluminium en poudre*

Mansour Issaoui [a, *], Lionel Limousy [b], Bénédicte Lebeau [b], Jamel Bouaziz [a], Mohieddine Fourati [a]

[a] *University of Sfax, National School of Engineers, Laboratory of Industrial Chemistry BP1173, Sfax, Tunisia*
[b] *University of Strasbourg, University of Haute-Alsace, Institute of Materials Science of Mulhouse (IS2M – UMR CNRS 7361), Mulhouse, France*

ARTICLE INFO

*Article history:*
Received 25 May 2015
Accepted 12 October 2015
Available online 6 February 2016

*Keywords:*
Kaolin
Porous supports
Aluminum powder
Surface charge
Wettability
Permeability

ABSTRACT

Porous flat ceramic-metal composite (Cermet) membrane supports were elaborated from kaolin and aluminum powder mixtures by the press drying–sintering process. The evolution of structure and surface properties was followed by water permeation, tensile strength, mercury porosimetry, surface charge and contact angle measurements. These characterizations have demonstrated that the addition of aluminum to the kaolin matrix has a beneficial effect on the membrane support properties. In particular, the water permeability and mechanical strength increased gradually in the presence of aluminum. In addition, the hydrophilicity of the cermet supports was found to increase gradually with the aluminum load. However, the surface charge was not affected by the aluminum introduced into the cermet composition. Filtration experiments were carried out with the support containing 4% wt of aluminum. The results have indicated that this support could be used to purify dye-containing water.



*Mots-clés:*
Kaolin
Supports poreux
Poudre d'aluminium
Charge de surface
Mouillabilité
Perméabilité

RÉSUMÉ

Des supports membranaires plans poreux céramique–métal (cermets) ont été élaborés par pressage d'une poudre sèche à partir d'un mélange de kaolin et d'aluminium. L'évolution de la structure et des propriétés de surface a été suivie par des mesures de perméabilité à l'eau, de résistance à la traction, de porosimètrie au mercure, de charge de surface et d'angle de contact. Ces caractérisations ont démontré que l'addition d'aluminium dans la matrice kaolinitique a un effet bénéfique sur les propriétés des supports membranaires. En particulier, la perméabilité à l'eau et la résistance mécanique ont augmenté progressivement en présence d'aluminium. En outre, l'hydrophilicité des supports céramique–métal a

* Corresponding author.
*E-mail address:* issaouimansour@yahoo.fr (M. Issaoui).

http://dx.doi.org/10.1016/j.crci.2015.10.011
1631-0748/

augmenté progressivement avec la teneur en aluminium. Toutefois, la charge de surface n'a pas été affectée par la présence de l'aluminium dans la composition du cermet. Les expériences de filtration ont été réalisées avec le support contenant 4% en masse d'aluminium. Les résultats ont montré que ce support peut être utilisé pour purifier l'eau contenant un colorant.



## 1. Introduction

A cermet is a composite material composed of ceramic (cer) and metallic (met) materials. It controls thermal expansion mismatch between the substrate and the functional coating. It acts as an intermediate coating material between the metallic bond coat and the ceramic top coat [1,2]. It presents several advantages, such as working under extreme conditions of temperature and chemical attack [3,4]. Cermets are used for instance as thermal barriers and thick clearance control coatings for turbine applications [1,2]. These composite materials, formed by using an insulating ceramic matrix and metallic particles, have recently received particular attention due to the singular combination of their mechanical and microstructural properties. Compared to their polymeric counterparts, porous ceramic composite membranes exhibit many excellent properties in the separation process, such as thermal and chemical stability [5]. As a consequence, the investigation on clays as membrane materials has attracted much attention.

In previous studies, composite membranes were generally manufactured from metallic oxides such as titania ($TiO_2$), alumina ($Al_2O_3$) [6] and Ni-alumina by different preparation methods, including soaking-rolling, electroless plating and impregnation [7,8]. Some efforts have been made to elaborate the porous ceramic support using kaolin as the main raw material [9,10]. This material which belongs to clay minerals has the advantage to be one of the most abundant minerals all over the world, which is cheap and easily accessible.

There are several approaches for the fabrication of porous ceramics. They can be produced by adding pore-forming agents into the starting powders, such as sawdust, starch, carbon or organic particulates [11], which after vaporization form homogeneous pores. Besides, the mixing of the ceramic powders with a bubble former was investigated. Generally, the obtained supports showed a number of shortcomings such as low porosity, small pore size, lower flow resistance, and high shrinkage [10]. It has been demonstrated that powders containing aluminum are cemented into a robust macroporous monolith during the hydrothermal oxidation [12]. Particularly, porous alumina ceramics are considered as reference supports for several mineral ultrafiltration membranes [13].

## 2. Materials and methods

### 2.1. Materials and chemicals

The raw materials were kaolin and aluminum powders obtained from BWW Minerals and Merck companies, respectively. After heating at 150 °C, the chemical analysis of kaolin was performed by using the X-ray fluorescence (XRF) technique using a PANalytical Magix model. The chemical composition given in weight percentages of oxides is listed in Table 1, in which the main impurities are $Fe_2O_3$, $K_2O$, MgO and CaO. For the aluminum powder, purity is more than 99%. All the materials were used as received.

**Table 1**
Chemical composition of the used kaolin (wt %).

| oxides | $SiO_2$ | $Al_2O_3$ | $Fe_2O_3$ | MgO | $K_2O$ | CaO | $TiO_2$ | LOI[a] |
|---|---|---|---|---|---|---|---|---|
| wt % | 47.85 | 37.60 | 0.83 | 0.17 | 0.97 | 0.57 | 0.74 | 11.27 |

[a] Loss on ignition.

The particle size distributions of kaolin and aluminum were determined using a Particle Sizing System Mastersizer Model 3000. The obtained results illustrated in Fig. 1 present an average particle size in the order of 8 μm and 121 μm, respectively.

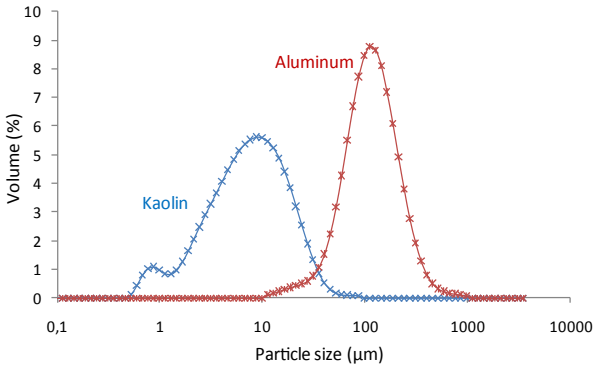


**Fig. 1.** Particle size distributions of the used kaolin and aluminum.

### 2.2. Elaboration of aluminum-kaolin membrane supports

The used procedure for the elaboration of aluminum-kaolin supports is as follows: several flat disks were prepared in a dry route, starting from kaolin powder homogeneously mixed with different ratios of aluminum powder (from 4 to 16 wt %) without the addition of water. The mixed powders were pressed uniaxially until 66 MPa with a compression rate of 2 $mm.mn^{-1}$, to get flat disks (30 mm

in diameter × 6 mm in thickness), which were then sintered using a programmable furnace at 1250 °C for 1 h with a heating rate of 5 °C $min^{-1}$.

### 2.3. Characterization techniques

Different techniques were used for the characterization of the raw materials and the prepared cermet supports namely: thermal analysis (DTA/TGA), mercury porosimetry, scanning electron microscopy (SEM), and water permeability, mechanical strength, surface charge and contact angle measurements.

The differential thermal analysis (DTA) and thermogravimetric analysis (TGA) were carried out from ambient temperature to 1300 °C at a rate of 10 °C $min^{-1}$ under air, using a Setaram instrument (SENSYS EVO 3D, Sensor Inside).

The mean pore size and pore size distribution of the sintered tubular supports were measured by mercury intrusion porosimetry, using an AutoPore IV Series 9500 from Micromeritics. This technique is based on the penetration of mercury into the solid pores as a function of pressure; the intrusion volume is recorded versus the applied pressure and then the pore size is determined. The pore size diameter $D$ (nm) was determined using the Washburn [14] (Eq. (1)):

$$D = \frac{-4\gamma \cos\theta}{P} \quad (1)$$

where $\gamma$ (dyn $cm^{-1}$) is the surface tension, $\theta$ (°) is the contact angle and $P$ (MPa) is the applied pressure. A contact angle of 130° and surface tension of 485 dyn $cm^{-1}$ were used. Porosities were calculated from Hg intrusion data.

SEM micrographs were taken from different samples using a PHILIPS XL30 apparatus, with an accelerating voltage of 7 kV. The samples were coated with a thin layer of gold before microscopy examination.

The open porosity of the sintered flat supports was measured by a water absorption test. The dry samples were weighed before the water absorption test, then wiped clean of all surface water after the water absorption test and weighed again. The open pore volume $V_{op}$ ($cm^3$) corresponds to the volume of water absorbed by the sample. Since the density of water is 1 g $cm^{-3}$ at 4 °C, the difference in weight (g) of the sample before and after saturation corresponds to the open pore volume:

$$V_{op} = m_s - m_d \quad (2)$$

where $m_s$ and $m_d$ are the mass (g) of the saturated and the dry samples, respectively. The percentage of the open porosity was calculated using the following formula:

$$\%\ Open\ porosity = 100\left(\frac{V_{op}}{V_a}\right) \quad (3)$$

where $V_{op}$ and $V_a$ are the open pore and the apparent volume of the samples ($cm^3$), respectively. This method has the advantages to measure only the accessible pores which are relevant to membrane transport, and to be a non-destructive technique.

The water permeability of the flat supports was characterized using a dead-end filtration apparatus (which will be described below) under transmembrane pressure (TMP) in the range from 1 to 6 bar at room temperature. Before each test, the concerned support was conditioned by immersion in distilled water for 24 h to reach a stable flux at the beginning of the experiment. The determination of the liquid permeability $Lp$ ($m^3\ m^{-2}$) was performed with distilled water, and calculated with Eq. (4) derived from Darcy's law [15, 16].

$$Lp = \frac{\mu.v}{\Delta P.\Delta t.s} \quad (4)$$

where $\mu$ (Pa.s), $v$ ($m^3$), $\Delta P$ (Pa), $\Delta t$ (s) and $s$ ($m^2$) are the dynamic viscosity, the runoff volume of liquid during the time $\Delta t$, the hydraulic pressure and the disk surface contact, respectively.

The tensile strength of the different cermet supports was calculated using a LLOYD EZ50 Instrument, measured by the Brazilian test applied to sintered flat disks with a displacement rate of 0.5 mm $min^{-1}$. The maximum rupture strength $\sigma_r$ (MPa) was determined following the elasticity theory [17]:

$$\sigma_r = \frac{2P_{max}}{\pi LD} \quad (5)$$

where $L$ (mm) and $D$ (mm) are the sample length and the diameter, respectively. $P_{max}$ (N) is the maximum applied load at failure. Three samples of each composition elaborated under the same conditions were tested and an average value was then calculated.

Zeta potential measurements were conducted using a Malvern Nanosizer instrument. The interest of these measurements lies in the determination of the IEP, where the permeation flux is maximal. It is also very useful to determine the sign of the surface charge at a given pH, allowing the measurement of the surface charge by absorbing the polyelectrolyte of the opposite charge (see SIP measurements described below). During these measurements, 20 mg of the powder of each support were dispersed in 50 mL of a $10^{-3}$ M NaCl solution. The pH of the suspension was adjusted using $10^{-1}$ M NaOH and/or HCl solutions and stirred for 24 h until ionic equilibrium was reached. Four measurements of the zeta potential ($\xi$ mV) were performed with each suspension and an average value was then calculated. Zeta potential measurements were achieved for pH values ranging from 3 to 11. For each support, the evolution of $\xi$ versus the pH was represented.

Streaming induced potential measurements were performed with a particle charge detector (PCD 03) μMütek device. The interest of this measurement is to observe the effect of different amounts of aluminum added inside the kaolin on the surface charge of the cermet. As an example, the modification of the surface charge may induce the adsorption of solutes on the surface of the cermet. During this characterization, 20 mg of each support (powder form) was dispersed in 50 mL of consequent polyelectrolyte (anionic/cationic) and stirred overnight. Then, 5 mL of each obtained suspension was introduced into the cylinder of the μMütek device. When the piston moved, it produced a

flowing potential that can be measured and displayed on the screen of the device.

In order to neutralize the excess of charge, the collected volume was directly titrated with a polyelectrolyte of reverse charge ($10^{-3}$ N polydiallyldimethylammonium chloride (Polydadmac: cationic polyelectrolyte) or sodium polyethylenesulfate (PesNa: anionic polyelectrolyte) solutions) to a streaming potential of 0 mV [18]. The net surface charge q (μequiv $g^{-1}$) of the support was calculated using Eq. (6):

$$q = \frac{(V_2 - V_1)\cdot C \cdot 1000}{W} \quad (6)$$

where $V_2$ is the required volume of the polyelectrolyte 2 to neutralize 5 mL of the polyelectrolyte used for the sample contact; $V_1$ is the volume of the polyelectrolyte 1 added for the background measuring out; $C$ is the concentration of the sample introduced into the initial 5 mL of solution used for the background measuring out; $W$ is the weight of the sample introduced into the initial 5 mL of solution used for the background measuring out.

The wettability character of the different supports was checked by measuring the contact angles of a water drop on the surface samples using an OCA 15EC Dataphysics goniometer. The angle is defined geometrically as the angle formed by a liquid at the three phase boundary where a liquid, gas and solid intersect. One advantage of this method is to be a non-destructive method for measuring the wetting of a solid by a liquid.

### 2.4. Compositions and sample designations

The compositions in wt % and the designations of the different membrane supports elaborated in this study are reported in Table 2.

**Table 2**
Compositions and sample designations of the supports.

| | Kaolin (wt %) | Aluminum (wt %) |
|---|---|---|
| Support 0 | 100 | 0 |
| Support 4 | 96 | 4 |
| Support 8 | 92 | 8 |
| Support 12 | 88 | 12 |
| Support 16 | 84 | 16 |

### 2.5. Experimental device used for the filtration tests

The filtration device used in this study was represented in a home-made pilot plant (Fig. 2). A disk-shaped support was sealed in a stainless steel module using O-rings. The purpose is to ensure a perpendicular direction of the liquid to the support surface (a dead-end filtration). The useful area of the membrane support is 5.54 $cm^2$. The transmembrane pressure (TMP) ranging between 1 and 10 bar was controlled by an adjustable valve at the outlet of the compressor. The liquid flux through the membrane support was measured as a function of time at different TMP values.

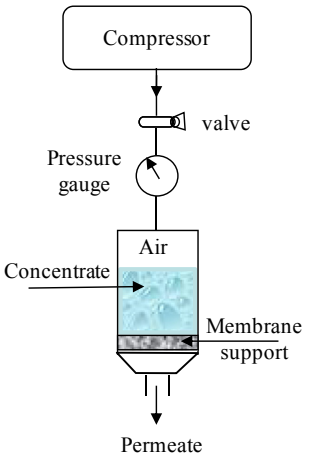


**Fig. 2.** Scheme of the pilot plant.

## 3. Results and discussion

### 3.1. Characterization of the starting materials

Both TGA and DTA characterizations were carried out simultaneously with the same device. The TGA-DTA curves recorded during the compact heating of the kaolin, aluminum, and kaolin/aluminum mixture are presented in Figs. 3 and 4.

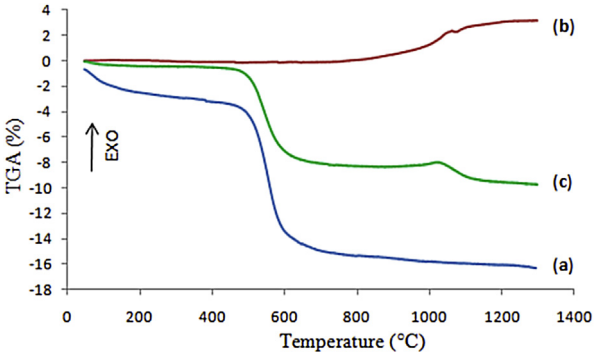


**Fig. 3.** TGA curves of the kaolin (a), aluminum (b) and kaolin/aluminum mixture (10 wt %, loose contact) (c).

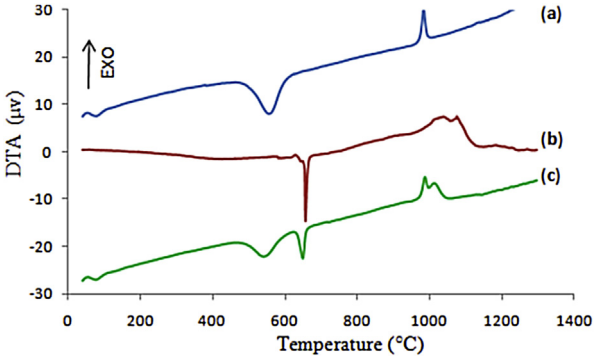


**Fig. 4.** DTA curves of the kaolin (a), aluminum (b) and kaolin/aluminum mixture (10 wt %, loose contact) (c).

The TGA curve of kaolin (Fig. 3a) shows a total weight loss of about 16%, which consists of two distinct stages. The first one between room temperature and 180 °C is due to the loss of physisorbed water. The second one in the temperature range of 400–800 °C is mainly caused by the dehydroxylation of the kaolinite. The DTA thermogram displayed in Fig. 4a shows two endothermic peaks at 70 °C and 540 °C associated with these two weight losses. The exothermic peak at 980 °C without any weight loss might be attributed to the crystallization of spinel or mullite [19].

From the DTA curve of the pure aluminum powder used in this study (Fig. 4b), it can be seen that the aluminum melting endotherm appears at a temperature around 660 °C, without significant modifications in the associated TGA (Fig. 3b). A weight gain of about 3.22% was observed from 660 °C to 1200 °C, which can be assigned to the liquid-state oxidation of aluminum characterized by an exothermic peak at 1030 °C in the DTA curve [20,21].

The addition of aluminum powder to the clay slightly modified its thermal behavior as it can be seen in the TGA-DTA curves of the mixture (kaolin/10 wt % aluminum) displayed in Figs. 3c and 4c, respectively. The total weight loss was reduced to about 10% compared to the one of the pure kaolin which was about 16%. Two steps are also observed, corresponding in this case to 3 phenomena: loss of physisorbed water in the 20–200 °C range, loss of water upon dehydroxylation in the 400–800 °C and gain of matter upon oxidation of aluminum in the 660–1200 °C range. The exothermic transformation of metakaolin is still observed at 980 °C.

### 3.2. Characterization of the elaborated cermet supports

The main properties of the fabricated porous cermet supports were characterized, including water permeability, mechanical strength, pore size distribution, SEM surface micrographs, surface charge and contact angle measurements.

#### 3.2.1. Mercury porosimetry and scanning electron microscopy

Mercury intrusion porosimetry was used initially to determine the influence of the aluminum content on the final pore size distributions of the elaborated cermet supports for membranes.

The cumulative pore volumes versus pore diameter curves for the ceramic supports with and without aluminum are presented in Fig. 5. The cumulative pore volume was found to increase with increasing percentage of aluminum, showing an increase in the pore size of the membrane supports. Such behavior is probably attributed to the exothermic oxidation reaction of aluminum which may provide energy for the germination of the α-alumina phase. The latter reacts with metakaolin to form the porous mullite phase. This reaction gives rise to bigger voids and pores [20]. The sample with 16 wt % Al showed higher porosity by exhibiting the highest cumulative pore volume compared to those elaborated with a lower percentage of aluminum. Consequently, this sample showed the highest intrusion mercury volume of about 0.3 mL $g^{-1}$.

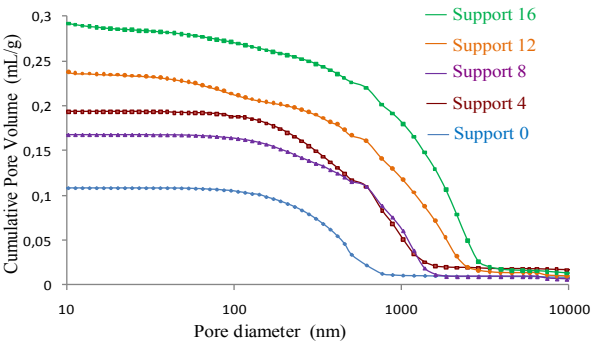


**Fig. 5.** Cumulative pore volume curves of the supports with and without aluminum, sintered at 1250 °C for 1 h.

The curves of the log differential pore volume calculated from the Washburn equation versus the mercury pressure of the samples are reported in Fig. 6. The curve enables to show that the flat ceramic support for the membrane prepared from kaolin alone displays a monomodal pore-size distribution corresponding to macropores with an average diameter of about 470 nm. This monomodal pore size distribution is usually obtained for samples having a uniform pore size distribution.

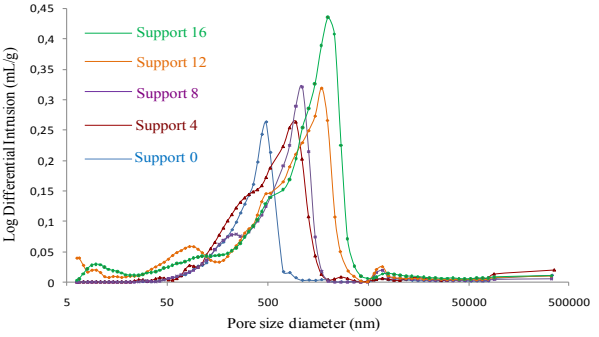


**Fig. 6.** Pore size distributions of the supports with and without aluminum, sintered at 1250 °C for 1 h.

The addition of aluminum leads to broader pore size distributions shifted to larger pores. The pore size distribution is multi-modal in the cermet samples with mean diameters of approximately 950, 1100, 1700 and 2000 nm for disks containing 4%, 8%, 12% and 16% of aluminum, respectively. The addition of aluminum in the kaolinitic matrix has a positive effect on void formation.

SEM images corresponding to the elaborated flat ceramic supports for membranes with and without aluminum are presented in Fig. 7. They show a broad distribution of voids and pores around a few microns, confirming the mercury intrusion data. These images should be taken with caution since they are not representative of the pore distribution presented above. These images demonstrate only that the presence of alumina leads to the formation of voids after sintering.

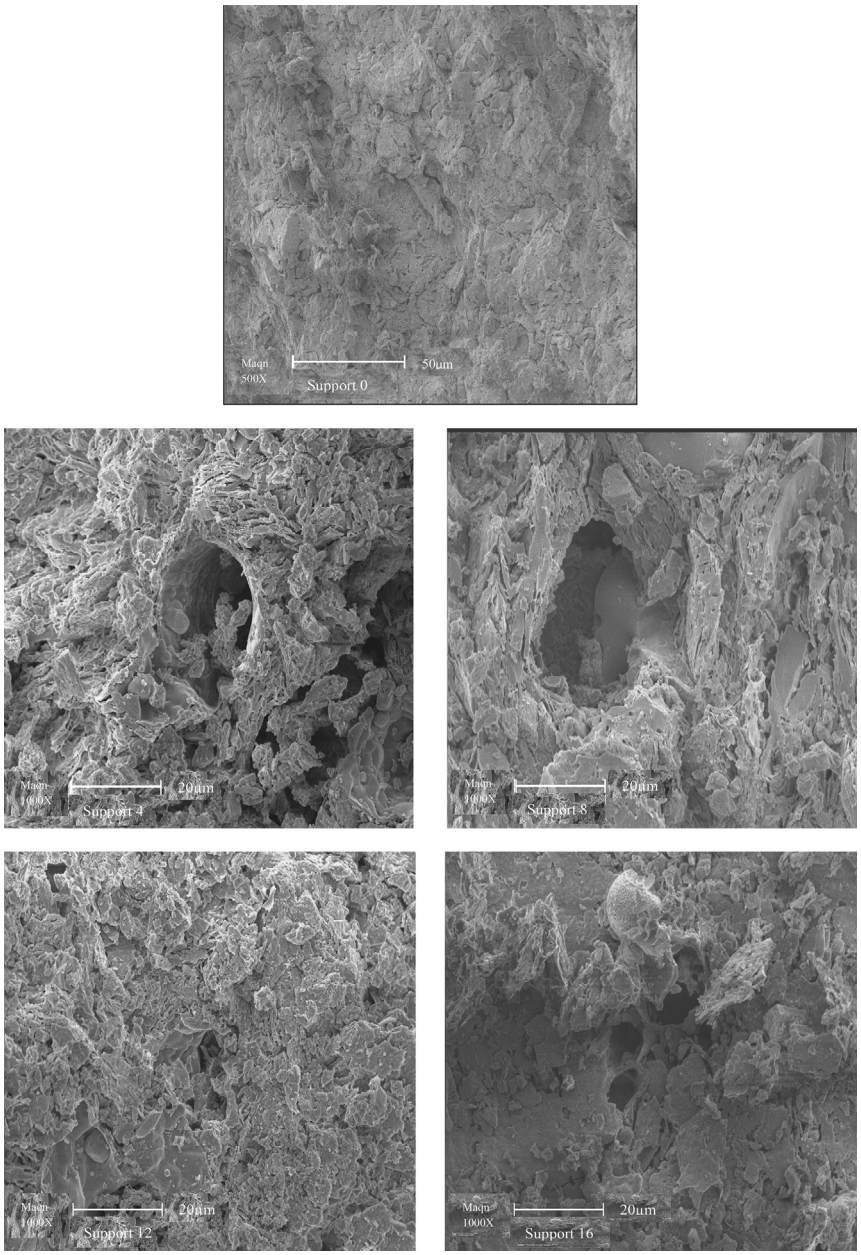


**Fig. 7.** Pore top-view SEM images of the flat supports with and without aluminum, sintered at 1250 °C for 1 h.

*3.2.2. Open porosity*

Fig. 8 shows the influence of the introduced aluminum in the open porosity of the ceramic supports with and without aluminum, sintered at 1250 °C for 1 h. The open porosity increases gradually with increasing amounts of metal in the kaolinitic matrix and reaches about 28.5% for the mixture with 16 wt % of aluminum. This can be due to bigger voids and pores created during the exothermic oxidation reaction of aluminum [20].

*3.2.3. Water permeability and mechanical strength*

For practical applications of the ceramic membranes, hydraulic permeability should be as high as possible and mechanical strength should be adjusted to the process specification. Therefore, in order to evaluate the influence of the added metal on the water permeability and mechanical characteristics of the cermet supports, samples were tested and results are shown in Fig. 9. As it can be seen, the water permeability of the supports elaborated with different wt % of aluminum increases slightly between 0 and 12%, but then increases sharply between 12 and 16%. It is clear that an increase of metal contents to the kaolinitic supports causes a higher flux. This is probably due to the exothermic oxidation reaction of aluminum which can produce germination of the α-aluminum phase that can react with the metakaolin to produce porous mullite. This

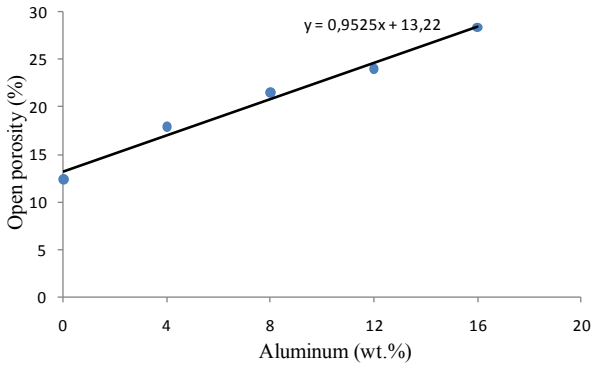


**Fig. 8.** Impact of the aluminum content inside the elaborated flat ceramic supports (sintered at 1250 °C for 1 h) on the open porosity.

reaction gives rise to bigger voids and pores in the elaborated cermet supports [22].

Good mechanical properties will also be necessary to withstand operating stresses. The rupture strength changes arbitrarily with the variation of the percentage of aluminum. The best mechanical properties are obtained for 4 wt % of metal doping in the kaolin matrix.

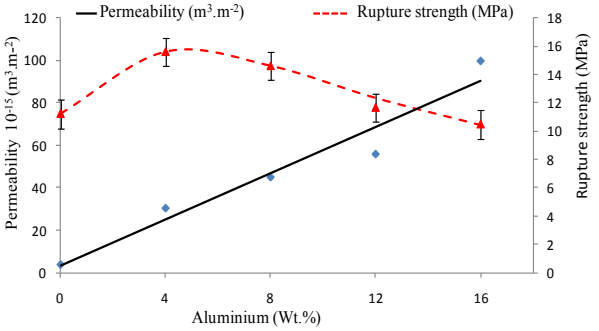


**Fig. 9.** Water permeability and rupture strength of the samples with different wt % of aluminum sintered at 1250 °C for 1 h.

### 3.2.4. Surface charge

*3.2.4.1. Qualitative determination of the surface charge.* The variation of zeta potential ξ of the elaborated flat supports for membranes as a function of pH is shown in Fig. 10. As it can be seen, the surface charge of all elaborated supports for membranes decreased with the increase in pH. For those prepared from kaolin alone, an IEP (isoelectric point) was reached at a pH close to 4. The addition of aluminum powder to the clay shifts the IEP to higher pH values, which were more than 7 for all samples containing the metal ranging from 4 to 16 wt %. This evolution corresponds to a change in the surface nature of cermet samples due to the presence of aluminum that tends to make the surface more basic. Cermets behave like $Al_2O_3$ and an impregnation with an anionic compound such as PES-Na is possible.

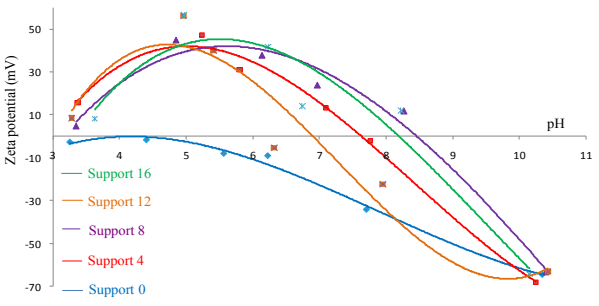


**Fig. 10.** Variation of ξ with the pH for samples containing different wt % of aluminum and sintered at 1250 °C for 1 h.

*3.2.4.2. Quantitative determination of the surface charge.* After having specified the sign of the surface charge of the elaborated supports for membranes, the surface charge values were estimated using the streaming induced potential methodology. The surface charge was calculated using Eq. (6) and the results are presented in Table 3.

**Table 3**
Surface charge of the samples sintered at 1250 °C for 1 h according to the pH with different wt % of aluminum.

| Aluminum content | 0% Al | 4% Al | 8% Al | 12% Al | 16% Al |
|---|---|---|---|---|---|
| pH | 7.18 | 7.17 | 7.26 | 7.34 | 7.44 |
| Surface charge (μequiv.g$^{-1}$) | −3.5 | +7 | +10.5 | +14.7 | +4.1 |

The membrane supports have very low surface charges even in the presence of aluminum. They are positively charged due to the incorporation of the aluminum powder. A low surface charge leads to the minimization of the electric and the dielectric effects, and then to the optimization of the flux of permeation. It may also avoid the formation of a polarization layer in the presence of ionic solutes.

### 3.2.5. Contact angle measurements

In order to explore the wettability properties of the surfaces of the elaborated supports for membranes, contact angle measurements were performed. These measurements are extremely sensitive to the physical and chemical composition of samples. They were performed by the sessile drop method using distilled water, and the results are shown in Fig. 11. The first observation shows that all the contact angles of the elaborated supports are lower than

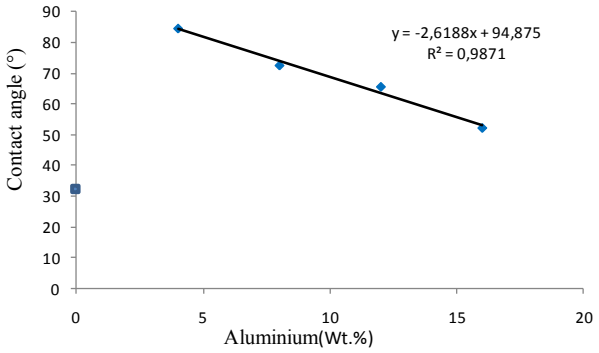


**Fig. 11.** Wetting angle measurements of samples with different wt % of aluminum sintered at 1250 °C for 1 h.

90°. They are characteristic of hydrophilic surfaces that are capable to absorb water [23]. These results suggest that the aluminum content in the cermet supports affects the hydrophilicity, and therefore the possibility of converting the hydrophilicity of the ceramic surfaces without chemical grafting. The addition of 4 %wt of alumina leads to a decrease of the surface hydrophilicity of the cermet, which favors the permeation of water through the support (minimization of the interaction between the support and the solvent).

### 3.3. Application to the treatment of a solution containing dyes

One of the most important industrial applications of the membrane separation process is the clarification of colored effluents coming out from many industrial processes [24, 25], like textile dye wastewater, which results in major environmental problems.

Hence, these porous flat cermet membrane supports were tested for the filtration of an Indigo blue solution with an initial concentration of dye equal to 2 g $L^{-1}$. All microfiltration experiments were carried out at a temperature of 25 °C and at a constant pressure of 6 bar, using the supports 0 and 4. Fig. 12 presents the evolution of the permeation flux during the filtration of the solution containing Indigo blue. As expected for the dead-end filtration process, the permeation flux decreases continuously during the experimentation and tends to stabilize at a flux close to 13 L $h^{-1}$ $m^{-2}$. The concentration of Indigo blue at the interface of the cermet membrane limits the mass transfer, leading to a decrease of the permeation flux (more than 40%). The preparation of the tubular cermet membrane will be considered in next studies to avoid this drawback and improve the filtration process.

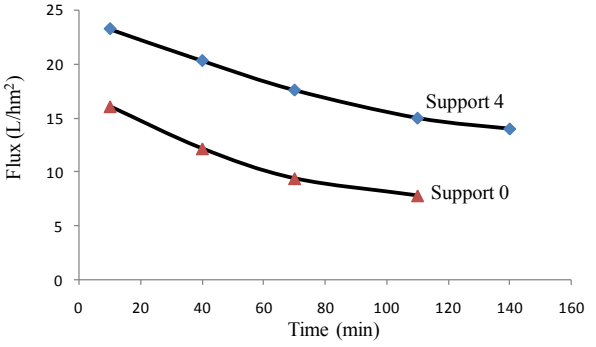


**Fig. 12.** Variations of permeate flux of Indigo blue solution with time ($T$ = 25 °C, TMP = 6 bar).

The results were evaluated through the observation of the retentate and the permeate colorations obtained during the filtration of the dyeing effluent (Fig. 13). The dead-end filtration process operating at an intermediate pressure (6 bar) was seen to remove quite completely the color of the parent solution (containing blue dye). It showed a significant retention of dyes in the concentrate and a complete discoloration of the starting solution. This final stage reached the maximum concentration of indigo for reuse.

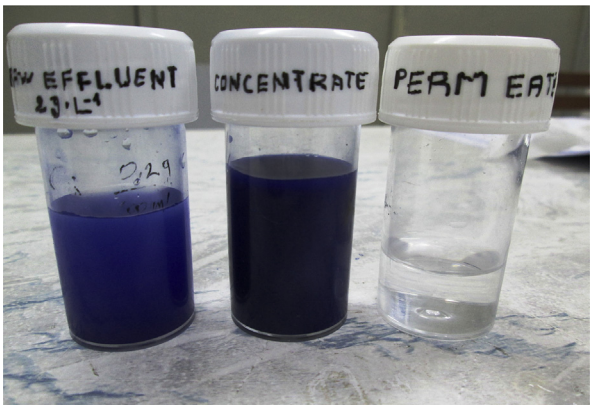


**Fig. 13.** Results of decolorization obtained after the filtration of an aqueous solution containing the Indigo blue dye ($T$ = 25 °C, $P$ = 6 bar): permeate solution (at the right), retentate (in the middle), and the initial solution (at the left).

## 4. Conclusion

Porous flat cermet membrane supports, based on kaolin and aluminum powder blends, were produced by dry molding. By introducing different amounts of metal, although mechanical properties, water permeability and wettability varied, the surface charge remains practically unalterable and low. The pure water permeability of the prepared samples sintered at 1250 °C for 1 h increases from $4.10^{-15}$ to about $1.10^{-13}$ $m^3$ $m^{-2}$ when the amount of aluminum was varied from 0 to 16 wt %. This modification is very interesting for the filtration process because the efficiency is estimated through the permeation flux. Indeed, the more the flux is, the more this process is profitable. The increase of metal content in the kaolin matrix has enhanced the mechanical strength of the sample containing 4% of the aluminum precursor (support 4), and leads to a contact angle of about 85°. The support 4 was used for the filtration of an industrial solution containing the Indigo blue dye. The obtained results have shown a total rejection of the dye, but a decrease of the permeation flux during the filtration process. This limitation of mass transfer can be avoided by using tubular cermet membranes. The first results obtained with this new type of ceramic membrane support are very promising for several reasons such as membrane selectivity, performances and cost. The development of new tubular supports will be investigated in further research studies with the possibility to commercialize new low cost ceramic ultrafiltration membranes.

## References

[1] J. Ilavsky, C.C. Berndt, Surf. Coat. Technol. 102 (1998) 19–24.
[2] R. Rajendran, Eng. Fail. Anal. 26 (2012) 355–369.
[3] A. Rajabi, M. Ghazali, S. Junaidi, A. Daud, Chem. Eng. J. 255 (2014) 445–452.
[4] N. Liu, Y. Xu, H. Li, M. Chen, J. Zhou, F. Xie, et al., J. Mater. Process Technol. 161 (2005) 478–484.
[5] R.R. Bhave, Inorganic Membranes: Synthesis, Characteristics and Applications, Van Nostrand Reinhold, New York, 1991, p. 10.

[6] T.V. Van Gestel, C. Vandecasteele, A. Buekenhoudt, C. Dotremont, J. Luyten, R. Leysen, B.V. der Bruggen, G. Maes, J. Membr. Sci. 207 (2002) 73–89.
[7] Y. Cy, S. Bk, L. Dw, P. Sj, L. Ky, L. Kh, J. Colloid Interface Sci. 319 (2008) 470.
[8] B. Ernst, S. Haag, M. Burgard, J. Membr. Sci. 288 (2007) 208–217.
[9] T. Mohammadi, A. Pak, Sep. Purif. Technol. 30 (2003) 241–249.
[10] B.K. Nandi, R. Uppaluri, M.K. Purkait, Appl. Clay. Sci. 42 (2008) 102.
[11] J.H. She, T. Ohji, Mater. Chem. Phys. 80 (2003) 610–614.
[12] S. Tikhov, Y. Potapova, V. Sadykov, V. Fenelonov, I. Yudaev, O. Lapina, A. Salanov, V. Zaikovskii, G. Litvak, Mater. Res. Innov. 9 (2005) 431–446.
[13] P.K. Lin, D.S. Tsai, J. Am. Ceram. Soc. 80 (1997) 365–372.
[14] E.W. Washburn, Proc. Natl. Acad. Sci. U.S.A 7 (1921) 115–116.
[15] P. Dutournié, L. Limousy, N. Zouaoui, H. Mahzoul, E. Chevereau, Desalination 280 (2011) 397–402.
[16] J. Bikaï, L. Limousy, P. Dutournié, L. Josien, W. Blel, C.R. Chimie 18 (2015) 56–62.
[17] S. Timoshenko, J.N. Goodier, Editorial Urmo, Bilbao, Spain, 1975.
[18] L. Limousy, H. Mahzoul, L. Hamon, B. Siffert, Colloids Surf. A: Physicochem. Eng. Aspects 181 (2001) 91–97.
[19] A. Yamuna, S. Devanarayanan, M. Lalithambika, J. Am. Ceram. Soc. 85 (2002) 1409–1413.
[20] T. Ebadzadeh, Ceram. Int. 31 (2005) 1091–1095.
[21] V. Viswabaskaran, F.D. Gnanam, M. Balasubramanian, Ceram. Int. 28 (2002) 557–564.
[22] M. Issaoui, J. Bouaziz, M. Fourati, Desalin Water Treat. 53 (2015) 1037–1044.
[23] R. Förch, H. Schönherr, A.T.A. Jenkins (Eds.), Surface design: applications in bioscience and nanotechnology, Wiley-VCH, Weinheim, Germany, 2009, p. 471.
[24] S. Chakraborty, S. De, J.K. Basu, S. DasGupta, Desalination 174 (2005) 73–85.
[25] C. Fersi, L. Gzara, M. Dhahbi, Desalination 185 (2005) 399–409.